Desalination and Water Treatment
www.deswater.com

doi: 10.5004/dwt.2023.29925

308 (2023) 244–251
October

Eosin Y removal using citric acid-treated corncob

Yinghua Song*, Shengming Chen, Hui Xu

Department of Chemistry and Chemical Engineering, Chongqing Technology and Business University, Chongqing 400067, China, Tel.: +86-023-62769785; Fax: +86-023-62769785; emails: yhswjyhs@126.com (Y.H. Song), chensm@ctbu.edu.cn (S.M. Chen), xuhui@ctbu.edu.cn (H. Xu)

Received 25 June 2023; Accepted 24 August 2023

ABSTRACT

In this study, citric acid-treated corncob (CATC) was used to remove Eosin Y (EY) from aqueous solutions by adsorption. The effects of initial solution pH, adsorbent particle size, contact time, and temperature on the adsorption of EY onto CATC were studied by static experiments. The Henry, Langmuir, and Freundlich isotherms were used to fit the equilibrium data. Pseudo-first-order, the pseudo-second-order, and Elovich models were used to test the kinetic data. It was found that the Henry and Freundlich isotherms gave a good description of the equilibrium process. The equilibrium capacity of 41.79 $mg \cdot g^{-1}$ was obtained for 300 $mg \cdot L^{-1}$ of EY concentration, pH = 4.0, a temperature of 323 K, and 2.5 $g \cdot L^{-1}$ of CATC dosage. Both the pseudo-second-order and Elovich models could provide a perfect fit for the kinetic data of the EY on the CATC, indicating that chemical interactions occur during adsorption. Based on the thermodynamic analysis, EY adsorption by CATC was endothermic and spontaneous. These findings suggested that CATC was highly promising as a low-cost and efficient adsorbent for the treatment of EY wastewater.

Keywords: Modified corncob; Eosin Y; Adsorption; Isotherm; Kinetics

1. Introduction

Large amounts of dye-containing wastewater come from many industries, including printing and dyeing, textiles, food, leather and paper, among others. Due to the high toxicity, teratogenicity, and carcinogenicity of such effluents, they have a serious impact on the environment and can endanger human health [1]. The dye-containing wastewater must be treated specially to reduce its harm to the environment before it is discharged. However, many dyes are difficult to degrade due to their complex aromatic ring structure. As a result, it has always been a headache to treat such dye-containing wastewater.

Among all kinds of physical and chemical treatment technologies for dye-containing wastewater, adsorption is superior to others because of its low cost, simple design, and easy operation [2]. At present, activated carbon is widely used in the treatment of dye-containing wastewater because of its high efficiency [3]. However, the processing costs are still relatively high. Researchers are developing cheaper and more effective alternatives from different raw materials to treat dye wastewater, such as banana peel [4], walnut shell [5], seaweed [6], mango pod [7], leaf powder [8], sawdust [9], rice husk [10], and orange peel [11], among others. These natural raw materials offer a new and efficient way for adsorption technology to achieve its goals of low cost and environmental friendliness.

As an agricultural by-product, corncob is often incinerated or simply discarded, creating large amounts of exhaust and dust that pose an environmental hazard. Because of its good adsorption property, high mechanical strength, good chemical stability, and low cost, it's considered to be an effective adsorbent for treating organic contaminants in wastewater, such as methyl red and methyl orange [12], methylene

* Corresponding author.

blue [13], bromocresol green [14], and crystal violet [15]. Suitable chemical modifications of the adsorbents have been shown to effectively increase the removal efficiency of dyes.

Activated carbon was prepared by chemical activation of corncob with concentrated H_3PO_4 to remove methylene blue and 17.57 mg·g^{-1} of maximum Langmuir adsorption capacity was achieved [16]. Nwadiogbu et al. [17] synthesized acetylated corncob with acetic anhydride to adsorb crude oil. They claimed that acetylation resulted in the maximum monolayer sorption capacities of the prepared hydrophobic corncobs increasing by almost 18 times in comparison with the raw corncobs. Ma et al. [18] studied the methylene blue adsorption using magnetic carbonaceous adsorbent derived from corncob. By carbonization under saline conditions and magnetization using iron(III) salt, the resultant adsorbent was synthesized. The resulting adsorbent exhibited a porous structure with a higher specific surface area and more oxygen-containing functional groups than their carbonaceous precursors. Corncob lignin was carbonized at 400°C and cross-linked with chitosan in the presence of epichlorohydrin to prepare a composite chitosan-biochar (CS-BC), and its adsorption capacity of CS-BC was increased by ~2 times when compared with unmodified biochar [19]. In another study, triethylenetetramine was used to bind with corncob biochar to produce nanobiochar-modified triethylenetetramine (NCB-TA), which was then treated with sulfuric acid to form positively charged nanobiochar-modified triethylenetetramine (NCB-TA-PC). This nano-biochar was successfully used to remove anionic dyes such as tartrazine and sunset yellow [20]. High removal rates of tartrazine and sunset yellow from actual water samples were obtained, with 93.73% and 95.42% from tap water. Moreover, researchers have discovered that the adsorption performance of the corncob towards cadmium(II) could be efficiently improved by citric acid modification [21]. The adsorption capacity of the modified corncob can be attributed to the carboxylic sites formed on the surface of natural corncob when the citric acid reacted with cellulose. During the chemical modification, each molecule of citric acid that binds to cellulose adds two more carboxylic sites to the corncob surface.

Eosin Y (EY) is a commonly used anionic dye known as Acid Red 87 with the formula $C_{20}H_6Br_4Na_2O_5$. Studies have shown that it is harmful to the skin and eyes. Adverse effects on vital organs like the liver and kidneys have also been reported as a result of dye ingestion [22].

In this study, citric acid was introduced to prepare a novel adsorbent citric acid-treated corncob (CATC) based on a raw corncob, and its removal ability of EY from aqueous solutions was studied depending on the initial solution pH, adsorbent particle size, contact time, EY concentration, and temperature. In addition, non-linear isotherm analysis and kinetic studies were performed to reveal the characteristics of EY adsorption on CATC. This work aims to develop a cost-effective and promising adsorbent from raw corncob for the removal of dyes from wastewater.

2. Materials and methods

2.1. Adsorbent

Raw corncob was prepared in Chongqing, China, from local markets as agricultural waste. It was soaked and washed thoroughly in deionized water to remove dust and water-soluble impurities, and dried in an oven at 60°C for 24 h, then grind into powder and sieved into different particle sizes for subsequent use.

The corncob was chemically modified with citric acid using a method similar to that proposed by Leyva-Ramos et al. [21]. A citric acid solution with a concentration of 0.2 M was prepared from reagent-grade monohydrated citric acid. The CATC was prepared by the following operations. 2.0 g of corncob and 125 mL of the citric acid solution were mixed in a flask and heated at 70°C for 3 h. Subsequently, the mixture was filtered and washed with deionized water several times until the pH of the effluent was no longer changing during washing. Finally, the prepared adsorbent was dried in an oven at 70°C for 24 h and then removed for use.

The EY stock solutions were prepared by dissolving 0.3 g of EY powder in 1,000 mL of deionized water, which was diluted to the desired concentrations (100–300 mg·L^{-1}) to obtain test solutions.

2.2. Adsorption studies

A certain volume of EY solution (100 mg·L^{-1}) was added in a conical flask with a volume of 250 mL, and the initial pH of the solution was then adjusted to a certain value with 1.0 mol·L^{-1} of sodium hydroxide or hydrochloric acid solution. After that, a certain amount of CATC was appended and stirred at a constant temperature (303–323 K) at 150 rpm until the equilibrium was reached. The residual EY concentration was determined at 515 nm spectrophotometrically (UV1102 Spectrophotometer, Techcomp, China) at regular time intervals. To ensure the accuracy of the data, the experiments were repeated, and the mean values were taken for subsequent calculations.

The amount of adsorption capacity q (mg·g^{-1}) was calculated using Eq. (1):

$$q = \frac{v\left(c_0 - c_t\right)}{m} \tag{1}$$

where c_0 (mg·L^{-1}) is the initial EY concentration, c_t (mg·L^{-1}) the concentration at time t, v (L) the solution volume, and m is the mass of the CATC (g).

The equilibrium and kinetic data were non-linearly fitted using the Microcal OriginPro 8.5.1 software.

3. Results and discussion

3.1. Characterization of CATC

3.1.1. Fourier-transform infrared spectroscopy

The Fourier-transform infrared (FTIR) spectra of the raw corncob, CATC and EY-loaded CATC are shown in Fig. 1. The spectra of the raw corncob and CATC presented similar characteristics and absorption peaks. This result could be attributed to similar functional groups in the raw corncob and citric acid. The observed characteristic band around 669 cm^{-1} can be assigned to C–OH bending. The strong and broad peak at 3,462 cm^{-1} could be assigned to the O–H groups, carboxylic groups or amide N–H stretching, corresponding to the vibration of functional groups in cellulose

or hemi-cellulose [23]. The peak located at 1,653 cm^{-1} was attributed to the stretching vibration of C=O in carboxylic acids and the intensity increased remarkably after treatment by citric acid, suggesting an increase in the number of carboxyl groups [24]. From this we can conclude that the raw corncob surface has been successfully modified by citric acid. The presence of a large number of carboxyl groups on the surface of the corncob may contribute to its increased adsorption capacity compared to the raw corncob.

Fig. 1 also shows the FTIR spectrum of the EY-loaded CATC. The intensity decreased when compared to that appeared in the FTIR spectra of CATC at 1,653 cm^{-1} showing the existence of electron acceptor-donor interaction between the carbonyl groups on the surface of the adsorbent and EY molecule [25]. The acid functional group in the case of adsorbent treated with citric acid is the –COOH group.

3.1.2. X-ray diffraction

The X-ray diffraction of CATC showed similar results to those of raw corncob with the same diffraction peak (Fig. 2). The most remarkable highlighted that characteristic sharp intensity diffraction peaks at 2θ values of 17°, 21.8° and 35° which reflect the crystalline nature of type I cellulose [15]. Treatment with citric acid did not alter the structure of cellulose.

3.2. Effect of initial solution pH

The effect of solution pH on EY adsorption using CATC has been examined based on the point of zero charges (pH_{pzc}) of CATC [15]. From Fig. 3 the pH_{pzc} of CATC was established to be 4.30. This implied that the CATC surface was positively charged when pH was less than pH_{pzc} = 4.30, and negatively charged when pH was greater than pH_{pzc} = 4.30 [26].

The adsorption capacity increased sharply when the initial solution pH increased from 2.0 to 4.0 and went down when the pH was greater than 4.0 (Fig. 4). At pH less than pH_{pzc} = 4.30, the CATC surface was highly occupied by the positively charged H^+ ions, which favored and enhanced the adsorption of the anion EY onto the CATC. At pH > pH_{pzc} = 4.30, the adsorption capacity decreased significantly as the number of negative charges on the CATC surface increased due to the electrostatic repulsion between the CATC surface and the negative EY species. Furthermore, the electrostatic adsorption of OH^- on CATC will also hinder the adsorption of the dye's anionic group. Similar results were found in anion dye adsorption on the macadamia seed husk [27].

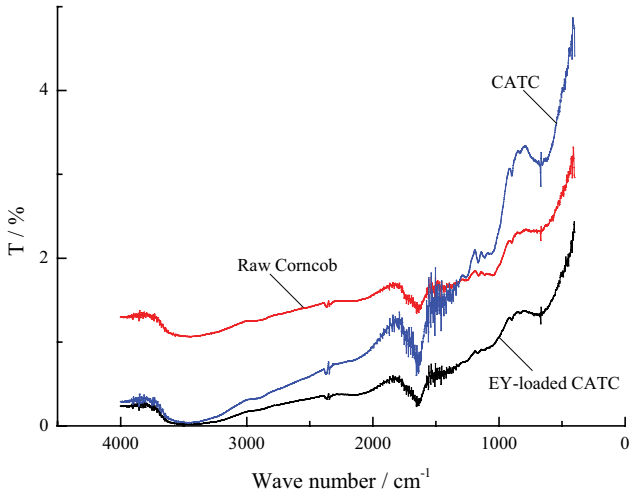

Fig. 1. Fourier-transform infrared spectroscopy of raw corncob, CATC and EY-loaded CATC.

3.3. Effect of CATC particle sizes

The adsorbent particle size can significantly affect the surface area available for adsorption. The larger the surface area of the adsorbent, the more adsorption sites, and the stronger the adsorption capability [27].

As shown in Fig. 5, the EY adsorption steadily increased as the size of the CATC particles decreased. For instance, the adsorption capacity increased from 7.41 to 13.63 $mg \cdot g^{-1}$ as the particle sizes decreased from 750~375 μm to 150–125 μm. This observation can be attributed to the larger surface area and therefore larger number of adsorption sites of the smaller CATC particles compared to larger ones. But if the size of the CATC particles is too small, the subsequent separation of the adsorbent from the solution becomes very difficult. Therefore, the particle size of

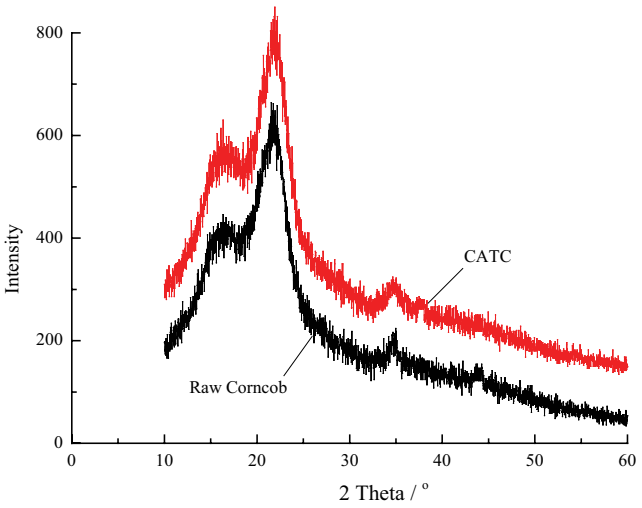

Fig. 2. X-ray diffractograms of raw corncob and CATC.

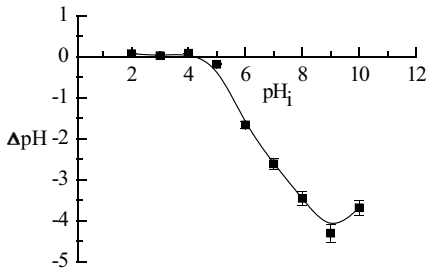

Fig. 3. The pH of the point of zero charges of CATC.

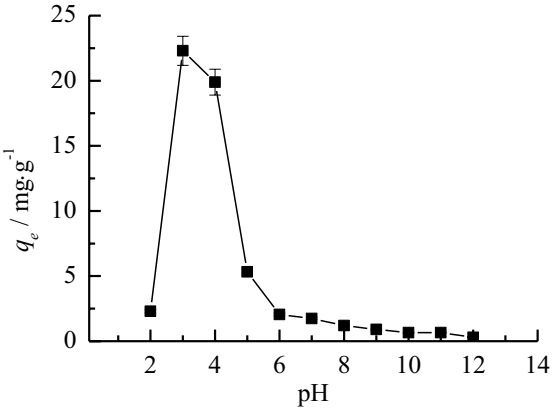

Fig. 4. Effect of pH (c_0 = 100 mg·L^{-1}, T = 303 K, CATC dosage = 1 g·L^{-1}, contact time = 6 h, rpm = 150).

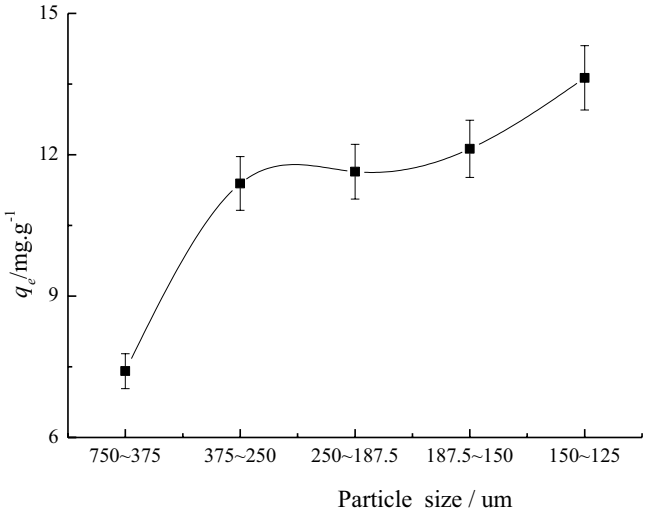

Fig. 5. Effect of CATC particle size (c_0 = 100 mg·L^{-1}, T = 303 K, pH = 4.0 ± 0.1, CATC dosage = 2.5 g·L^{-1}, contact time = 5 h, rpm = 150).

375~250 μm was chosen in further studies. These results were consistent with related research on the adsorption of crystal violet onto coffee husks [28].

3.4. Effect of contact time and temperature

The adsorption of EY on CATC was investigated at the concentration of 100 mg·L^{-1} and the temperature of 303, 313, and 323 K, respectively (Fig. 6). At the same concentration, the equilibrium adsorption capacity of EY on CATC increased slightly with the increase in temperature (from 11.65 mg·g^{-1} at 303 K to 12.25 mg·g^{-1} at 323 K), which indicated that EY adsorption on CATC was an endothermic process. The increased capacity with increasing temperature can be attributed to the increased mobility of the EY molecules and the reduced viscosity of the aqueous solution allowing more EY molecules to interact with the active sites on the CATC surface. At the same time, this was also due to the fact that the force between the EY molecule and the active adsorption site on the CATC surface was larger than

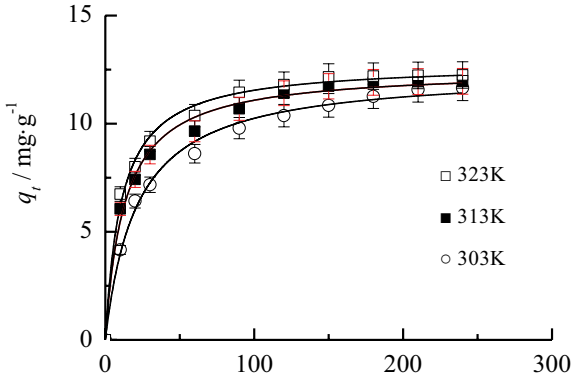

Fig. 6. Effect of contact time (c_0 = 100 mg·L^{-1}, pH = 4.0 ± 0.1, CATC dosage = 2.5 g·L^{-1}, rpm = 150). The lines represented the best non-linear regression fits with the pseudo-second-order kinetics.

the force between the EY molecule and the solvent. A similar result has been previously reported in the adsorption of crystal violet onto a composite adsorbent [29].

It is clear from Fig. 6 that EY removal proceeded very rapidly for the first 100 min, then slowly decreased, and finally reached equilibrium around 300 min. At first, the adsorption of EY proceeded very quickly because there were many vacant adsorption sites on the surface of the CATC. As these vacancies were occupied, the adsorption rate gradually decreased. Over time, the repulsive force between the bulk solution and the EY molecule increased, hindering the adsorption of EY on the remaining vacancy sites. Similar findings were also obtained for the adsorption of Acid Orange 7 and Basic Red 5 by activated carbon [30].

3.5. Adsorption isotherms

The Henry (linear), Langmuir (non-linear), and Freundlich (non-linear) isotherms were used to describe the equilibrium system.

$$q_e = K_H c_e \tag{2}$$

$$q_e = \frac{q_{\max} K_L C_e}{1 + K_L C_e} \tag{3}$$

$$q_e = k_F C_e^{1/n} \tag{4}$$

where C_e (mg·L^{-1}) is the equilibrium EY concentration, q_e (mg·L^{-1}) and $q_{\max}$ (mg·L^{-1}) the equilibrium and the maximum Langmuir adsorption capacity, respectively, K_H the linear distribution coefficient of Henry equation, K_L and k_F (L·mg^{-1}) the Langmuir and the Freundlich equilibrium constant, n (dimensionless) a constant related to the heterogeneity of the adsorbent.

As shown in Fig. 7, with the increase of EY concentration, the adsorption capacity of EY on CATC increased from 9.18 to 33.9 mg·g^{-1} at 303 K, from 9.69 to 37.49 mg·g^{-1} at 313 K, and from 10.19 to 41.79 mg·g^{-1} at 323 K. At the same temperature, as the initial EY concentration increased, the mass transfer driving force increased, and the interaction force between EY and CATC was enhanced, thus

increasing the adsorption capacity of CATC. The results were in agreement with those described for the adsorption of Victoria Blue B onto Indian jujube seeds [31]. The equilibrium adsorption capacity also increased with temperature for the same concentration, as shown in Fig. 7. Similar results were obtained in the adsorption of crystal violet onto sugarcane bagasse [32].

Equilibrium data were used to analyze the adsorption process using the above isothermal models. The correlation parameters for the Henry and Freundlich isotherms are listed in Table 1. Although the determined coefficients R^2 for the Langmuir model were greater than 0.98, both K_L and q_{max} were less than zero for different temperatures. Therefore, the Langmuir isotherm was not considered suitable for the simulation of EY adsorption by CATC, and the corresponding fitted data are not given in Table 1. The non-linear fits with the Freundlich isotherm for the adsorption of EY on CATC is shown in Fig. 7. Based on the simulation results in Table 1, the adsorption equilibrium of EY onto CATC was well described by the Henry and Freundlich isotherms. Henry's law holds for adsorption on a homogeneous surface at sufficiently low concentrations. The Freundlich isotherm is used for heterogeneous surfaces. However, it was observed that the "1/*n*" values for the Freundlich model were close to 1. When the "1/*n*" value is fairly close to 1, the Freundlich isotherm can be simplified to the Henry model with linear equilibrium data. Fig. 7 shows that the EY equilibrium data exhibited a similar behavior to the Henry isotherm. This behavior indicated that the equilibrium concentration is insufficient for the available adsorption sites on the CATC surface to be fully occupied by EY. Similar results can be found in the studies of methylene blue adsorption by calcinated diatomite [33] and the Yellow 194 adsorption by tannery solid waste [34].

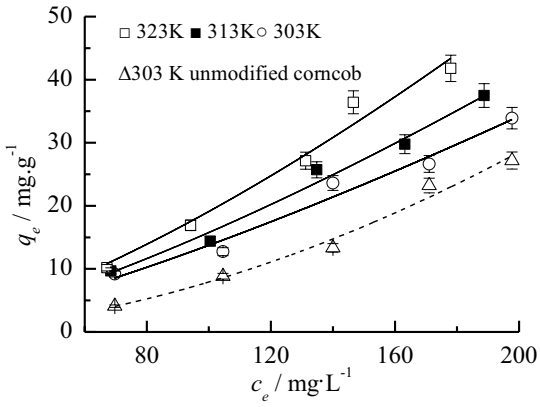

Fig. 7. Adsorption isotherms of EY onto CATC. (pH = 4.0 ± 0.1, adsorbent dosage = 2.5 g·L^{-1}, contact time = 5 h, rpm = 150). The lines represented the non-linear fits with the Freundlich isotherm model.

Table 1
Isotherms constants for the adsorption of EY on CATC

T (K)	Henry constants		Freundlich constants		
	K_D	R^2	K_F (10^{-2})	1/*n*	R^2
303	0.18	0.9871	3.24	0.76	0.9670
313	0.16	0.9874	2.98	0.73	0.9812
323	0.22	0.9814	2.73	0.70	0.9682
303[a]	0.12	0.9490	0.158	0.54	0.9782

[a]Equilibrium data of unmodified corncob.

To compare the adsorption properties on the raw corncob, the equilibrium adsorption of EY on the raw corncob at 303 K was investigated (Fig. 7) and the fitting results were also given in Table 1. Compared with the raw corncob, the adsorption capacity of EY on CATC was significantly improved, which could be confirmed by increased k_F values from 1.58×10^{-3} to 3.24×10^{-2} (Table 1) due to the enhanced interaction force between EY and the adsorbent.

The Langmuir maximum EY adsorption capacity of different adsorbents was compared in Table 2. q_e of CATC for EY was 41.79 mg·g^{-1}, which was comparable to other adsorbents. CATC has the potential to be a promising adsorbent for dye removal from aqueous solutions. However, adsorbents with lower or higher q_{max} than CATC such as cellulose acetate-montmorillonite composite [35], sugarcane bagasse modified with tetraethylenepentamine [39], are expensive as compared to the cheap corncob, and also their preparation methods are more complex.

Table 2
Comparison of adsorption capacities of various adsorbents for EY

Absorbent	Langmuir q_{max} (mg·g^{-1})	*T* (°C)	References
Cellulose acetate-montmorillonite composite	0.35	60	[35]
De-oiled soya	7.61	40	[36]
Lemon peel	8.24	30	[37]
Unmodified corncob	21.18[b]	30	Present work
CATC	41.79[a]	50	Present work
CNT/$ZnCo_2O_4$	141.09	25	[22]
Trimethylammonium grafted cellulose foams	364.22	30	[38]
Sugarcane bagasse modified with tetraethylenepentamine	399.04	25	[39]
Polyaniline coated lignocellulose	533.9		[40]

[a]Equilibrium data of CATC;
[b]Equilibrium data of unmodified corncob.

3.6. Adsorption kinetics

The kinetic behavior of EY adsorption by CATC was investigated using the pseudo-first-order [41], pseudo-second-order [42], and the Elovich models [43].

$$q_t = q_e\left(1 - e^{-k_1 t}\right) \tag{5}$$

$$q_t = \frac{k_2 q_e^2 t}{1 + k_2 q_e t} \tag{6}$$

$$q_t = \frac{1}{\beta}\ln(\alpha\beta) + \frac{1}{\beta}\ln(t) \tag{7}$$

where q_e (mg·g^{-1}) is the calculated equilibrium capacity. k_1 (min^{-1}) the rate constant for the first-order, k_2 (g·mg^{-1}·min^{-1}) the rate constant for the second-order models, α (mg·g^{-1}·min^{-1}) the initial desorption rate, and β is (g·mg^{-1}) the Elovich desorption constant.

The non-linear fit of the pseudo-second-order model is shown in Fig. 6. The results of the fits for these models are shown in Table 3 together with the determined coefficients R^2. Considering the very low value of R^2, and the large difference between the equilibrium adsorption capacity simulated by the model and the experimental data, the pseudo-first-order kinetic model was not suitable to describe EY adsorption on CATC. At three temperatures, the correlative coefficients obtained by the pseudo-second-order kinetics were all close to 1 (>0.99), and the q_e values calculated with the pseudo-second-order kinetics were much close to the experimental data. These results indicated that the pseudo-second-order model could well represent the adsorption kinetics of EY on CATC. This was further supported by the finding of Pandey et al. [44] where pine needle biomass was used for methylene blue adsorption. Since all R^2 values were greater than 0.99, the Elovich model could also provide a perfect description of the EY adsorption onto the CATC. Given this, chemical interactions based on electron exchange or charge sharing occurred between EY and CATC during this process. This was in agreement with the previous study of methylene blue adsorption by corncob [45].

3.7. Thermodynamic parameters

Standard free energy changes ΔG, enthalpy changes ΔH, and entropy changes ΔS as the thermodynamic parameters were calculated with the help of Eq. (8) [46].

$$\Delta G = \left(\Delta H - T\Delta S\right) = -RT\ln K_e \tag{8}$$

where K_e is the equilibrium constant (dimensionless).

The key factor in determining the thermodynamic parameters with Eq. (8) is the correct calculation of K_e, which has been estimated using different methods. But from Eq. (8) we can see that K_e should be a dimensionless parameter. The Freundlich equilibrium constant K_F can be converted to a dimensionless K_e with Eq. (8) when K_F was expressed as (mg·g^{-1})(L·mg^{-1})$^{1/n}$ [47]. This calculation method was recommended to be more accurate than the direct use of K_F [48]. K_e calculated with Eq. (8) is listed in Table 4.

$$K_e = K_F\rho\left(\frac{10^6}{\rho}\right)^{\left(1-\frac{1}{n}\right)} \tag{9}$$

where ρ is the density of pure water (~1.0 g·mL^{-1}).

The negative ΔG values derived from the constants K_e (dimensionless) revealed a spontaneous process and the increase in magnitude with the increasing temperature showed that the process was more favored at higher temperature [49]. The positive ΔH values proved that the adsorption of EY onto CATC was endothermic, which was consistent with the experimental data. The calculated

Table 4
Thermodynamic properties of this system

T (K)	K_e	ΔG (kJ·mol^{-1})	ΔH (R^2) (kJ·mol^{-1})	ΔS (J·mol^{-1}·K^{-1})
303	1.02	–0.06		
313	1.24	–0.56	21.20 (0.9745)	69.96
323	1.72	–1.46		

Table 3
Statistical results of the application of the kinetic models

Model			Temperature (K)		
			303	313	323
Pseudo-first-order	k_1	Rate constant, min^{-1}	1.95	2.40	2.01
	$q_{e,cal}$	Equilibrium capacity, mg·g^{-1}	9.19	10.14	10.64
	R^2	Determined coefficient	0.5222	0.662	0.7108
Pseudo-second-order	k_2 (10^{-3})	Rate constant, g·mg^{-1}·min^{-1}	3.77	6.17	7.27
	$q_{e,cal}$	Equilibrium capacity, mg·g^{-1}	12.43	12.52	12.79
	R^2	Determined coefficient	0.9935	0.9913	0.9937
Elovich	α	Rate constant, mg·g^{-1}·min^{-1}	1.61	4.75	8.34
	β	Elovich constant, g·mg^{-1}	0.43	0.51	0.55
	R^2	Determined coefficient	0.9973	0.9954	0.9929
$q_{e,exp}$		Experimental data of the equilibrium capacity, mg·g^{-1}	12.26	12.59	12.90

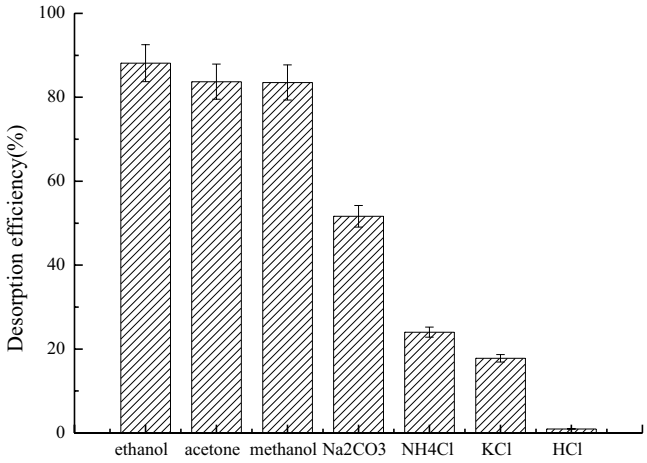

Fig. 8. Desorption.

positive values for ΔS reflected the affinity EY-CATC and increased randomness on the CATC surface. Similar results were reported in the adsorption of Erythrosine B [50].

3.8. Desorption study

To evaluate the reuse of CATC, different eluents were used to elude the EY adsorbed on CATC, including 1 M HCl, 1 M KCl, 1 M NH_4Cl, 1 M methanol, 1 M ethanol, 1 M acetone, and 1 M Na_2CO_3. Fig. 8 shows that 88.14%, 83.73%, 83.54%, 51.64%, 24.02%, 17.80%, and 0.97% of the adsorbed EY was desorbed with ethanol, acetone, methanol, Na_2CO_3, NH_4Cl, KCl, and HCl, respectively in the first cycle. It appeared that ethanol presents the highest desorption efficiency at 88.14%, indicating that the CATC had a good regeneration capacity for EY adsorption.

4. Conclusions

Corncob treated with citric acid was used as an adsorbent to remove EY from aqueous media. It was demonstrated that the adsorption capacity of EY was affected by the size of the adsorbent particles, the initial solution pH value, the temperature, and the initial EY concentration. The equilibrium and kinetic data obtained were analyzed using two-parameter non-linear models. It was shown that the Henry and Freundlich isotherms gave a good description of the adsorption equilibrium data. Both the pseudo-second-order and Elovich models are able to provide a perfect fit to the kinetic data, indicating that chemical interactions occur between the CATC surface and the EY molecules during adsorption. CATC can be used as a low-cost and highly effective adsorbent for EY removal.

Acknowledgment

This work was supported by the Project Foundation of the Chongqing Municipal Education Committee (KJ1600619).

References

[1] A. Rubio-Clemente, J. Gutiérrez, H. Henao, A.M. Melo, J.F. Pérez, E. Chica, Adsorption capacity of the biochar obtained from *Pinus patula* wood micro-gasification for the treatment of polluted water containing malachite green dye, J. King Saud Univ. Eng. Sci., (2021), doi: 10.1016/j.jksues.2021.07.006 (in Press).
[2] A. Ahmad, S.H. Mohd-Setapar, C.S. Chuong, A. Khatoon, W.A. Wani, R. Kumar, M. Rafatullah, Recent advances in new generation dye removal technologies: novel search for approaches to reprocess wastewater, RSC Adv., 5 (2015) 30801–30818.
[3] R. Davarnejad, S. Afshar, P. Etehadfar, Activated carbon blended with grape stalks powder: Properties modification and its application in a dye adsorption, Arabian J. Chem., 3 (2020) 5463–5473.
[4] A.A. Oyekanmi, A. Ahmad, K. Hossain, M. Rafatullah, Adsorption of Rhodamine B dye from aqueous solution onto acid treated banana peel: response surface methodology, kinetics and isotherm studies, PLoS One, 14 (2019) e0216878, doi: 10.1371/journal.pone.0216878.
[5] Y.H. Song, R. Peng, L.L. Gou, M. Ye, Removal of sunset yellow by methanol modified walnut shell, Iran. J. Chem. Chem. Eng., 40 (2021) 1095–1104.
[6] M. Yadav, S. Thakore, R. Jadeja, Removal of organic dyes using *Fucus vesiculosus* seaweed bio-adsorbent an ecofriendly approach: equilibrium, kinetics and thermodynamic studies, Environ. Chem. Ecotoxicol., 4 (2022) 67–77.
[7] K.A. Adegoke, O. Adeleke, M.O. Adesina, R.O. Adegoke, O.S. Bello, Clean technology for sequestering Rhodamine B dye on modified mango pod using artificial intelligence techniques, Curr. Res. Green Sustainable Chem., 5 (2022) 100275, doi: 10.1016/j.crgsc.2022.100275.
[8] B. Geremew, D. Zewde, *Hagenia abyssinica* leaf powder as a novel low-cost adsorbent for removal of methyl violet from aqueous solution: optimization, isotherms, kinetics, and thermodynamic studies, Environ. Technol. Innovation, 28 (2022) 102577, doi: 10.1016/j.eti.2022.102577.
[9] S. Bhowmik, V. Chakraborty, P. Das, Batch adsorption of indigo carmine on activated carbon prepared from sawdust: a comparative study and optimization of operating conditions using response surface methodology, Results Surf. Interfaces, 3 (2021) 100011, doi: 10.1016/j.rsurfi.2021.100011.
[10] K.K. Hummadi, S. Luo, S.B. He, Adsorption of methylene blue dye from the aqueous solution *via* bio-adsorption in the inverse fluidized-bed adsorption column using the torrefied rice husk, Chemosphere, 287 (2022) 131907, doi: 10.1016/j.chemosphere.2021.131907.
[11] Y.H. Song, R. Peng, S.M. Chen, Malachite green adsorption from aqueous solution by epichlorohydrin-modified orange peel, Fresenius Environ. Bull., 30 (2021) 4569–4577.
[12] S.J. Salih, A.S.A. Kareem, S.S. Anwer, Adsorption of anionic dyes from textile wastewater utilizing raw corncob, Heliyon, 8 (2022) e10092, doi: 10.1016/j.heliyon.2022.e10092.
[13] Y. Miyah, A. Lahrichi, M. Idrissi, Removal of cationic dye-methylene blue-from aqueous solution by adsorption onto corn cob powder calcined, J. Mater. Environ. Sci., 7 (2016) 96–104.
[14] C.E. Onu, P.E. Ohale, B.N. Ekwueme, I.A. Obiora-Okafo, C.F. Okey-Onyesolu, C.P. Onu, C.A. Ezema, O.O. Onu, Modeling, optimization, and adsorptive studies of bromocresol green dye removal using acid functionalized corn cob, Cleaner Chem. Eng., 4 (2022) 100067, doi: 10.1016/j.clce.2022.100067.
[15] Y.H. Song, R. Peng, S.M. Chen, Y.Q. Xiong, Adsorption of crystal violet onto epichlorohydrin-modified corncob, Desal. Water Treat., 154 (2019) 376–384.
[16] G.O. El-Sayed, M.M. Yehia, A.A. Asaad, Assessment of activated carbon prepared from corncob by chemical activation with phosphoric acid, Water Resour. Ind., 7–8 (2014) 66–75.
[17] J.O. Nwadiogbu, V.I.E. Ajiwe, P.A.C. Okoye, Removal of crude oil from aqueous medium by sorption on hydrophobic corncobs: equilibrium and kinetic studies, J. Taibah Univ. Sci., 10 (2016) 56–63.
[18] H. Ma, J.-B. Li, W.-W. Liu, M. Miao, B.-J. Cheng, S.-W. Zhu, Novel synthesis of a versatile magnetic adsorbent derived from corncob for dye removal, Bioresour. Technol., 190 (2015) 13–20.

[19] X.-J. Liu, M.-F. Li, J.-F. Ma, J. Bian, F. Peng, Chitosan crosslinked composite-based on corncob lignin biochar to adsorb methylene blue: kinetics, isotherm, and thermodynamics, Colloids Surf., A, 642 (2022) 128621, doi: 10.1016/j.colsurfa.2022.128621.
[20] M.E. Mahmoud, A.M. Abdelfattah, R.M. Tharwat, G.M. Nabil, Adsorption of negatively charged food tartrazine and sunset yellow dyes onto positively charged triethylenetetramine biochar: optimization, kinetics and thermodynamic study, J. Mol. Liq., 318 (2020) 114297, doi: 10.1016/j.molliq.2020.114297.
[21] R. Leyva-Ramos, L.E. Landin-Rodriguez, S. Leyva-Ramos, N.A. Medellin-Castillo, Modification of corncob with citric acid to enhance its capacity for adsorbing cadmium(II) from water solution, Chem. Eng. J., 80 (2012) 113–120.
[22] I.A. Lawal, T.H. Dolla, K. Pruessner, P. Ndungu, Synthesis and characterization of deep eutectic solvent functionalized CNT/$ZnCo_2O_4$ nanostructure: kinetics, isotherm and regenerative studies on Eosin Y adsorption, J. Environ. Chem. Eng., 7 (2019) 102877, doi: 10.1016/j.jece.2018.102877.
[23] R. Gnanasambandam, A. Proctor, Determination of pectin degree of esterification by diffuse reflectance Fourier-transform infrared spectroscopy, Food Chem., 15 (2000) 327–332.
[24] S.K. Ghosh, A. Bandyopadhyay, Adsorption of methylene blue onto citric acid-treated carbonized bamboo leaves powder: equilibrium, kinetics, thermodynamics analyses, J. Mol. Liq., 248 (2017) 413–424.
[25] A. Essekri, M.A. Haki, M. Laabd, A.A. Addi, R. Lakhmiri, A. Albourine, Citric acid-functionalized Acacia pods as a robust biosorbent for decontamination of wastewater containing crystal violet dye: experimental study combined with statistical optimization, Chem. Eng. Res. Des., 195 (2023) 390–403.
[26] O.A.A. Eletta, O.A. Ajayi, O.O. Ogunleye, I.C. Akpan, Adsorption of cyanide from aqueous solution using calcinated eggshells: equilibrium and optimization studies, J. Environ. Chem. Eng., 4 (2016) 1367–1375.
[27] M.M. Felista, W.C. Wanyonyi, G. Ongera, Adsorption of anionic dye (Reactive black 5) using macadamia seed husks: kinetics and equilibrium studies, Sci. Afr., 7 (2020) e00283, doi: 10.1016/j.sciaf.2020.e00283.
[28] G.K. Cheruiyot, W.C. Wanyonyi, J.J. Kiplimo, E.N. Maina, Adsorption of toxic crystal violet dye using coffee husks: equilibrium, kinetics and thermodynamics study, Sci. Afr., 5 (2019) e00116, doi: 10.1016/j.sciaf.2019.e00116.
[29] M. Sulyman, J. Kucinska-Lipka, M. Sienkiewicz, A. Gierak, Development, characterization and evaluation of composite adsorbent for the adsorption of crystal violet from aqueous solution: isotherm, kinetics, and thermodynamic studies, Arabian J. Chem., 4 (2021) 103115, doi: 10.1016/j.arabjc.2021.103115.
[30] S. Bouzikri, N. Ouasfi, L. Khamliche, *Bifurcaria bifurcata* activated carbon for the adsorption enhancement of Acid Orange 7 and Basic Red 5 dyes: kinetics, equilibrium and thermodynamics investigations, Energy Nexus, 77 (2022) 100138, doi: 10.1016/j.nexus.2022.100138.
[31] T.A. Khan, Md. Nouman, D. Dua, S.A. Khan, S.S. Alharthi, Adsorptive scavenging of cationic dyes from aquatic phase by H_3PO_4 activated Indian jujube (*Ziziphus mauritiana*) seeds based activated carbon: isotherm, kinetics, and thermodynamic study, J. Saudi Chem. Soc., 26 (2022) 101417, doi: 10.1016/j.jscs.2021.101417.
[32] A.S. Omer, G.A. El Naeem, A.I. Abd-Elhamid, O.O.M. Farahat, A.A. El-Bardan, H.M.A. Soliman, A.A. Nayl, Adsorption of crystal violet and methylene blue dyes using a cellulose-based adsorbent from sugarcane bagasse: characterization, kinetic and isotherm studies, J. Mater. Res. Technol., 9 (2022) 3241–3254.
[33] M.A.M. Khraisheh, M.A. Al-Ghouti, S.J. Allen, M.N. Ahmad, Effect of OH and silanol groups in the removal of dyes from aqueous solution using diatomite, Water Res., 39 (2005) 922–932.
[34] J.S. Piccin, C.S. Gomes, L.A. Feris, M. Gutterres, Kinetics and isotherms of leather dye adsorption by tannery solid waste, Chem. Eng. J., 183 (2012) 30–38.
[35] M. Goswami, A.M. Das, Synthesis and characterization of a biodegradable cellulose acetate-montmorillonite composite for effective adsorption of Eosin Y, Carbohydr. Polym., 206 (2019) 863–872.
[36] A. Mittal, D. Jhare, J. Mittal, Adsorption of hazardous dye Eosin Yellow from aqueous solution onto waste material de-oiled soya: isotherm, kinetics and bulk removal, J. Mol. Liq., 179 (2013) 133–140.
[37] A. Bukhari, I. Ijaz, H. Zain, E. Gilani, A. Nazir, A. Bukhari, S. Raza, J. Ansari, S. Hussain, S.S. Alarfaji, R. Saeed, Y. Naseer, R. Aftab, S. Iram, Removal of Eosin dye from simulated media onto lemon peel-based low cost biosorbent, Arabian J. Chem., 15 (2022) 103873, doi: 10.1016/j.arabjc.2022.103873.
[38] C. Feng, P. Ren, M. Huo, Z. Dai, D. Liang, Y. Jin, F. Ren, Facile synthesis of trimethylammonium grafted cellulose foams with high capacity for selective adsorption of anionic dyes from water, Carbohydr. Polym., 241 (2020) 116369, doi: 10.1016/j.carbpol.2020.116369.
[39] G.-B. Jiang, Z.-T. Lin, X.-Y. Huang, Y.-Q. Zheng, C.-C. Ren, C.-K. Huang, Z.-J. Huang, Potential biosorbent based on sugarcane bagasse modified with tetraethylenepentamine for removal of Eosin Y, Int. J. Biol. Macromol., 50 (2012) 707–712.
[40] S. Debnath, N. Ballav, A. Maity, K. Pillay, Single stage batch adsorber design for efficient Eosin yellow removal by polyaniline coated lignocellulose, Int. J. Biol. Macromol., 72 (2015) 732–739.
[41] S. Lagergren, About the theory of so-called adsorption of soluble substances, Kungliga Svenska Vetenskapsakademiens, Handlingar, 24 (1898) 1–39.
[42] Y.S. Ho, G. McKay, Pseudo-second-order model for sorption processes, Process Biochem., 34 (1999) 451–465.
[43] R. Nodehi, H. Shayesteh, A.R. Kelishami, Enhanced adsorption of congo red using cationic surfactant functionalized zeolite particles, Microchem. J., 153 (2020) 104281, doi: 10.1016/j.microc.2019.104281.
[44] D. Pandey, A. Daverey, K. Dutta, V.K. Yata, K. Arunachalam, Valorization of waste pine needle biomass into biosorbents for the removal of methylene blue dye from water: kinetics, equilibrium and thermodynamics study, Environ. Technol. Innovation, 25 (2022) 102200, doi: 10.1016/j.eti.2021.102200.
[45] A. Medhat, H.H. El-Maghrabi, A. Abdelghany, N.M. Abdel Menem, P. Raynaud, Y.M. Moustafa, M.A. Elsayed, A.A. Nada, Efficiently activated carbons from corn cob for methylene blue adsorption, Appl. Surf. Sci. Adv., 3 (2021) 100037, doi: 10.1016/j.apsadv.2020.100037.
[46] F. Naghmeh, T. Majid, H. Samaneh, Selective adsorption of Mo(VI) ions from aqueous solution using a surface-grafted Mo(VI) ion imprinted polymer, Polymer, 144 (2018) 80–91.
[47] H.N. Tran, S.-J. You, H.-P. Chao, Thermodynamic parameters of cadmium adsorption onto orange peel calculated from various methods: a comparison study, J. Environ. Chem. Eng., 4 (2016) 2671–2682.
[48] H.N. Tran, S.-J. You, A. Hosseini-Bandegharaei, H.-P. Chao, Mistakes and inconsistencies regarding adsorption of contaminants from aqueous solutions: a critical review, Water Res., 120 (2017) 88–116.
[49] R. Khamirchi, A. Hosseini-Bandegharaei, A. Alahabadi, S. Sivamani, A. Rahmani-Sani, T. Shahryari, I. Anastopoulos, M. Miri, H.N. Tran, Adsorption property of Br-PADAP-impregnated multiwall carbon nanotubes towards uranium and its performance in the selective separation and determination of uranium in different environmental samples, Ecotoxicol. Environ. Saf., 150 (2018) 136–143.
[50] C.C. Okoye, O.D. Onukwuli, C.F. Okey-Onyesolu, Utilization of salt activated *Raphia hookeri* seeds as biosorbent for Erythrosine B dye removal: kinetics and thermodynamics studies, J. King Saud Univ. Sci., 31 (2019) 849–858.